COMPDYN 2015
5th ECCOMAS Thematic Conference on
Computational Methods in Structural Dynamics and Earthquake Engineering
M. Papadrakakis, V. Papadopoulos, V. Plevris (eds.)
Crete Island, Greece, 25–27 May 2015

A MODE SELECTION ALGORITHM FOR THE FLEXIBILITY-BASED COMPONENT MODE SYNTHESIS

Jin-Gyun Kim[1], Phill-Seung Lee[2], and Kwang-Chun Park[3]

[1] Korea Institute of Machinery and Materials

156, Gajeongbuk-ro, Yuseong-gu, Daejeon 305-343, Republic of Korea

jingyun@kimm.re.kr

[2] Division of Ocean Systems Engineering, Korea Advanced Institute of Science and Technology

291, Daehak-ro, Yuseong-gu, Daejeon 305-701, Republic of Korea

phillseung@kaist.edu

[3] Department of Aerospace Engineering Sciences and Center for Aerospace Structures, University of Colorado Boulder

Campus Box 429, Boulder, CO 80309, U.S.A

kcpark@colorado.edu

Keywords: Component mode synthesis; Mode selection; Error estimation; Computational dynamics; Finite element method

Abstract. *A major challenge in component mode synthesis (CMS) remains the absence of a robust mode selection algorithm which can provide a measure of accuracy of the reduced model compared to the full model. In order to address this challenge, two concepts have been proposed in tandem: mode selection and error estimation methods. In this paper, we reassess performance of a recently proposed mode selection method and an a posteriori error estimation method, and propose an efficient iterative algorithm that combines these two methods. The flexibility-based component mode synthesis (F-CMS) is used to demonstrate the performance of the above methods. Numerical examples illustrate the effectiveness of the present algorithm.*

1 INTRODUCTION

Component mode synthesis (CMS) is a popular reduced-order modeling technique of the large finite element model in computational dynamics. After introducing the first approach of the CMS method in 1960s, various methods have been proposed [1-12]. In particular, the flexibility based CMS (F-CMS) method was developed using localized Lagrange multipliers [13], and its extended works have been performed [14,15].

In CMS methods, since the reduced order model is constructed by assembling substructural modes, its accuracy depends on the selection of dominant substructural modes. Generally, the frequency cut-off rule has been used to select the substructural modes [15-17], and it relies on the basic assumption of the mode superposition which the lower substructural modes contribute more to the lower global modes. While the frequency cut-off rule is simple and easy to use, this assumption is not always true in the CMS methods. For the reason, Park and Park developed a new mode selection method using residual interface flexibility in the F-CMS method [12]. Also, Kim et al. [17] have developed another mode selection method based on the eigenvector relation between substructural and global modes, and it shows better performance than previous ones but also is applicable to various CMS methods such as Craig-Bampton (CB) and Automated multi-level substructuring (AMLS) methods. In addition, Kim and Lee recently developed new error estimation methods to directly estimate the relative eigenvalue error [18-20] unlike the previous methods [9, 21, 22]. In this paper, we propose an iterative mode selection algorithm that combines the mode selection and error estimation methods developed by Kim et al. [17, 20], and its feasibility is studied using the F-CMS method.

First, we introduce the F-CMS method in Section 2. The mode selection and error estimation methods are presented in Section 3. A new mode selection algorithm and its performances are presented in Sections 4 and 5, respectively. The conclusions are given in Section 6.

2 FLEXIBILITY BASED CMS (F-CMS) METHOD

The displacement-based discrete energy functional $\Pi(\mathbf{u}_g)$ of the global structure is

$$\Pi(\mathbf{u}_g) = \mathbf{u}_g^T\left(\frac{1}{2}\mathbf{K}_g\mathbf{u}_g - \mathbf{f}_g + \mathbf{M}_g\ddot{\mathbf{u}}_g\right),\ \mathbf{M}_g = \mathbf{L}^T\mathbf{M}_s\mathbf{L},\ \mathbf{K}_g = \mathbf{L}^T\mathbf{K}_s\mathbf{L}, \tag{1}$$

where $\mathbf{M}_g$ and $\mathbf{K}_g$ are global mass and stiffness matrices, respectively, and $\mathbf{u}_g$ and $\mathbf{f}_g$ are global displacement and force vectors. $\mathbf{M}_s$ and $\mathbf{K}_s$ are block diagonal mass and stiffness matrices of substructures. The substructures and global structure are related with an assembly Boolean matrix $\mathbf{L}$. Using $\delta\Pi(\mathbf{u}_g)$, the eigenvalue problem is obtained

$$\mathbf{K}_g(\boldsymbol{\varphi}_g)_i = \lambda_i\mathbf{M}_g(\boldsymbol{\varphi}_g)_i,\ i = 1, 2, ..., N_g,\ \mathbf{u}_g = \boldsymbol{\Phi}_g\mathbf{q}_g, \tag{2}$$

where λ_i and $(\boldsymbol{\varphi}_g)_i$ are the eigenvalue and eigenvector, respectively. N_g is the number of DOFs in the global model. $\boldsymbol{\Phi}_g$ and $\mathbf{q}_g$ are the global eigenvector matrix and generalized coordinate vector, respectively. Using the localized Lagrange multipliers $\boldsymbol{\lambda}_\ell$, Equation (1) can be redefined as the sum of the substructural and constraint energy functionals

$$\Pi(\mathbf{u}_s,\ \boldsymbol{\lambda}_\ell, \mathbf{u}_b) = \mathbf{u}_s{}^T\left(\frac{1}{2}\mathbf{K}_s\mathbf{u}_s - \mathbf{f}_s + \mathbf{M}_s\ddot{\mathbf{u}}_s\right) + \boldsymbol{\lambda}_\ell\left(\mathbf{B}^T\mathbf{u}_s - \mathbf{L}_b\mathbf{u}_b\right), \tag{3}$$

in which $\mathbf{u}_s$ and $\mathbf{f}_s$ are the displacement and force vectors of the substructures, respectively, $\mathbf{u}_b$ is the interface displacement vectors, and $\mathbf{B}$ denotes the interface Boolean matrix. $\mathbf{L}_b$ is

obtained by yanking out the rows with zero entries of $\mathbf{B}^T\mathbf{L}$. When $\mathbf{u}_s$ is decomposed by deformable and rigid body modes, Equation (1) can be expressed by $\Pi(\mathbf{q}_s, \boldsymbol{\alpha}_s, \boldsymbol{\lambda}_\ell, \mathbf{u}_b)$, which yields

$$\begin{bmatrix} \boldsymbol{\Phi}_s^T\mathbf{K}_s\boldsymbol{\Phi}_s + \boldsymbol{\Phi}_s^T\mathbf{M}_s\boldsymbol{\Phi}_s\dfrac{d^2}{dt^2} & \mathbf{0} & \boldsymbol{\Phi}_s^T\mathbf{B} & \mathbf{0} \\ \mathbf{0} & \mathbf{R}_s^T\mathbf{M}_s\mathbf{R}_s\dfrac{d^2}{dt^2} & \mathbf{R}_s{}^T\mathbf{B} & \mathbf{0} \\ \mathbf{B}^T\boldsymbol{\Phi}_s & \mathbf{B}^T\mathbf{R}_s & \mathbf{0} & -\mathbf{L}_b \\ \mathbf{0} & \mathbf{0} & -\mathbf{L}_b^T & \mathbf{0} \end{bmatrix} \begin{bmatrix} \mathbf{q}_s \\ \boldsymbol{\alpha}_s \\ \boldsymbol{\lambda}_\ell \\ \mathbf{u}_b \end{bmatrix} = \begin{bmatrix} \boldsymbol{\Phi}_s^T\mathbf{f}_s \\ \mathbf{R}_s^T\mathbf{f}_s \\ \mathbf{0} \\ \mathbf{0} \end{bmatrix}, \tag{4}$$

where $\boldsymbol{\Phi}_s$ and $\mathbf{R}_s$ are the eigenvector matrices of the deformable and rigid body modes of substructures, and the corresponding generalized coordinate vectors are denoted by $\mathbf{q}_s$ and $\boldsymbol{\alpha}_s$. It should be noted that $\boldsymbol{\Phi}_s$ and $\mathbf{R}_s$ are calculated from the substructural eigenvalue problem using $\mathbf{M}_s^{(k)}$ and $\mathbf{K}_s^{(k)}$ ($k = 1,2,...,N_s$). Here, N_s denotes the number of substructures. Then, $\boldsymbol{\Phi}_s$ can be divided as

$$\boldsymbol{\Phi}_s\,\mathbf{q}_s = \boldsymbol{\Phi}_d\,\mathbf{q}_d + \boldsymbol{\Phi}_r\,\mathbf{q}_r, \tag{5}$$

where subscripts d and r denote the dominant and residual terms, respectively. To construct the effective reduced model, only dominant substructural modes are retained. Substituting Equation (5) into Equation (4) and performing the Gauss elimination on $\mathbf{q}_r$, the condensed equations are obtained. Finally, we have the final reduced eigenvalue problem

$$\overline{\mathbf{K}}_p(\overline{\boldsymbol{\varphi}}_p)_i = \overline{\lambda}_i\overline{\mathbf{M}}_p(\overline{\boldsymbol{\varphi}}_p)_i,\ i = 1,2,...,\overline{N}_p,\ \overline{\mathbf{u}}_p = \overline{\boldsymbol{\Phi}}_p\overline{\mathbf{q}}_p, \tag{6}$$

$$\overline{\mathbf{K}}_p = \begin{bmatrix} \boldsymbol{\Phi}_d^T\mathbf{K}_s\boldsymbol{\Phi}_d & \mathbf{0} & \boldsymbol{\Phi}_d^T\mathbf{B} & \mathbf{0} \\ \mathbf{0} & \mathbf{0} & \mathbf{R}_s{}^T\mathbf{B} & \mathbf{0} \\ \mathbf{B}^T\boldsymbol{\Phi}_d & \mathbf{B}^T\mathbf{R}_s & -\mathbf{F}_{rbs} & -\mathbf{L}_b \\ \mathbf{0} & \mathbf{0} & -\mathbf{L}_b^T & \mathbf{0} \end{bmatrix},\ \overline{\mathbf{M}}_p = \begin{bmatrix} \boldsymbol{\Phi}_d^T\mathbf{M}_s\boldsymbol{\Phi}_d & \mathbf{0} & \mathbf{0} & \mathbf{0} \\ \mathbf{0} & \mathbf{R}_s^T\mathbf{M}_s\mathbf{R}_s & \mathbf{0} & \mathbf{0} \\ \mathbf{0} & \mathbf{0} & \mathbf{F}_{rbm} & \mathbf{0} \\ \mathbf{0} & \mathbf{0} & \mathbf{0} & \mathbf{0} \end{bmatrix},$$

$$\overline{\boldsymbol{\Phi}}_p = \left[\overline{\boldsymbol{\Phi}}_{q_d}{}^T \quad \overline{\boldsymbol{\Phi}}_{\alpha_s}{}^T \quad \overline{\boldsymbol{\Phi}}_{\lambda_\ell}{}^T \quad \overline{\boldsymbol{\Phi}}_{u_b}{}^T\right]^T, \tag{7a}$$

$$\mathbf{F}_{rbs} = \mathbf{B}^T\mathbf{M}_s^{-1/2}[\mathbf{M}_s^{-1/2}\mathbf{K}_s\mathbf{M}_s^{-1/2}]^+\mathbf{M}_s^{-1/2}\mathbf{B} - \boldsymbol{\Phi}_{db}\boldsymbol{\Lambda}_d^{-1}\boldsymbol{\Phi}_{db}^T, \tag{7b}$$

$$\mathbf{F}_{rbm} = \mathbf{B}^T\mathbf{M}_s^{-1/2}[\mathbf{M}_s^{-1/2}\mathbf{K}_s\mathbf{M}_s^{-1/2}]^{+2}\mathbf{M}_s^{-1/2}\mathbf{B} - \boldsymbol{\Phi}_{db}\boldsymbol{\Lambda}_d^{-2}\boldsymbol{\Phi}_{db}^T, \tag{7c}$$

where $\overline{\mathbf{M}}_p$ and $\overline{\mathbf{K}}_p$ are the reduced partitioned mass and stiffness matrices, respectively, and $\overline{\lambda}_i$ and $(\overline{\boldsymbol{\varphi}}_p)_i$ are the approximated global eigenvalue and eigenvector, respectively. $\mathbf{F}_{rbs}$ and $\mathbf{F}_{rbm}$ are the static and dynamic parts of residual flexibility. Here, $\overline{N}_p$ is the number of DOFs in the reduced model ($\overline{N}_p << N_g$).From the third row in Equation (7a), $\overline{\boldsymbol{\Phi}}_g$ is computed by

$$\boldsymbol{\Phi}_g \approx \overline{\boldsymbol{\Phi}}_g = \mathbf{L}\overline{\boldsymbol{\Phi}}_{u_b} = \boldsymbol{\Phi}_d\overline{\boldsymbol{\Phi}}_{q_d} + \mathbf{R}_s\overline{\boldsymbol{\Phi}}_{\alpha_s} - \hat{\mathbf{F}}_r\mathbf{B}\overline{\boldsymbol{\Phi}}_{\lambda_\ell}. \tag{8}$$

3 PREREQUISITES FOR THE MODE SELECTION ALGORITHMS

3.1 Mode selection method

The mode selection method developed by Kim et al. [17] is based on the relation between the substructural and global eigenvectors. $\boldsymbol{\Phi}_d\overline{\boldsymbol{\Phi}}_{q_d}$ in Equation (8) means a direct link between

the substructural and the global eigenvectors. Therefore, $\overline{\mathbf{\Phi}}_{q_d}$ is regarded as a relation matrix between the approximate global eigenvector matrix $\overline{\mathbf{\Phi}}_g$ and the dominant substructural eigenvector matrix $\mathbf{\Phi}_d$. Consequently, $\overline{\mathbf{\Phi}}_{q_d}$ can be utilized as an indicator of the contributions of the dominant substructural modes to the global modes.

In order to calculate the substructural modal contribution, we first construct a trial intermediate reduced model denoted by a tilde $(\tilde{\cdot})$, and it contains more substructural modes than the final reduced model. The numbers of the selected substructural modes for the intermediate and final reduced models are defined by $\tilde{N}_d$ and $\overline{N}_d$ ($\overline{N}_d < \tilde{N}_d$), respectively. Then, a relation matrix $\tilde{\mathbf{\Phi}}_{q_d}$ could be calculated solving the eigenvalue problem of the intermediate reduced model. $\left(\tilde{\phi}_{q_d}^{(k)}\right)_{ij}$ is a component of $\tilde{\mathbf{\Phi}}_{q_d}$ corresponding to the contribution of the ith substructural mode in the kth substructure to the jth global mode, and then the magnitude of each row of $\tilde{\mathbf{\Phi}}_{q_d}$ for a substructure implies the contribution level of the corresponding substructural mode to the global modes in $\overline{\mathbf{\Phi}}_g$. Then, the substructural modal contributions can be calculated as

$$C_i^{(k)} = \sqrt{\sum_{j=1}^{\tilde{N}_p} \left[\kappa_j \left(\tilde{\phi}_{q_d}^{(k)}\right)_{ij}\right]^2}, \tag{9}$$

where $C_i^{(k)}$ is an indicator of the contribution of the ith substructural mode of the kth substructure, and here κ_j denotes the weighting factor with the following rule

$$\kappa_j = 1 \text{ for } N_t^L \le j \le N_t^U, \text{ otherwise } \kappa_j = 0, \tag{10}$$

in which N_t^L and N_t^U denote the lower and upper limits of the target global modes, respectively. Both mode numbers are used to define the range of the target global modes.

3.2 Error estimation method

We here introduce the recently proposed error estimation method [20] that is another priority of the mode selection algorithm. Since λ_i and $(\boldsymbol{\varphi}_g)_i$ are the exact eigensolutions of the global eigenvalue problem in Equation (2), the following equations should be satisfied

$$\frac{1}{\lambda_i}(\boldsymbol{\varphi}_g)_i^T \mathbf{K}_g (\boldsymbol{\varphi}_g)_i = (\boldsymbol{\varphi}_g)_i^T \mathbf{M}_g (\boldsymbol{\varphi}_g)_i. \tag{11}$$

Here, the exact global eigensolutions are expressed by the approximated terms and the error terms $\delta\lambda_i$ and $(\delta\boldsymbol{\varphi}_g)_i$

$$\lambda_i = \overline{\lambda}_i + \delta\lambda_i, \ (\boldsymbol{\varphi}_g)_i = (\overline{\boldsymbol{\varphi}}_g)_i + (\delta\boldsymbol{\varphi}_g)_i, \tag{12}$$

and also, we assume that $\mathbf{K}_g$ can be divided as the approximated and its error matrices as

$$\mathbf{K}_g = \overline{\mathbf{K}}_g + \delta\mathbf{K}_g \ \text{ with } (\overline{\boldsymbol{\varphi}}_g)_k^T \overline{\mathbf{K}}_g (\overline{\boldsymbol{\varphi}}_g)_k = \overline{\lambda}_k, \tag{13}$$

in which $\delta\mathbf{K}_g$ is error in the global stiffness matrix. Using Equations (12) and (13) in Equation (11), we have

$$\frac{\overline{\lambda}_i}{\lambda_i} - (\overline{\boldsymbol{\varphi}}_g)_i^T \mathbf{M}_g (\overline{\boldsymbol{\varphi}}_g)_i = \frac{1}{\lambda_i}(\delta\boldsymbol{\varphi}_g)_i^T \left[\mathbf{K}_g - \lambda_i \mathbf{M}_g\right](\delta\boldsymbol{\varphi}_g)_i - \frac{1}{\lambda_i}(\overline{\boldsymbol{\varphi}}_g)_i^T \delta\mathbf{K}_g (\overline{\boldsymbol{\varphi}}_g)_i. \tag{14}$$

If the approximated global eigenvector $(\overline{\boldsymbol{\varphi}}_g)_i$ is close enough to the exact global eigenvector $(\boldsymbol{\varphi}_g)_i$, the right-hand side in Equation (14) that are much smaller than the terms in the left-hand side can be negligible. Consequently, Equation (14) can be rewritten by

$$\frac{\overline{\lambda}_i}{\lambda_i} - 1 \approx (\overline{\boldsymbol{\varphi}}_g)_i^T \mathbf{M}_g (\overline{\boldsymbol{\varphi}}_g)_i - 1, \tag{15}$$

where the left-hand side in Equation (15) is the relative eigenvalue error, and the right-hand side is the mass-orthonormality error of the approximated global eigenvector $(\overline{\boldsymbol{\varphi}}_g)_i$. This derivation procedure shows that the mass-orthonormality error is a direct approximation of the relative eigenvalue error. Then, we define the error estimation parameter η_i as

$$\eta_i = (\overline{\boldsymbol{\varphi}}_g)_i^T \mathbf{M}_g (\overline{\boldsymbol{\varphi}}_g)_i - 1. \tag{16}$$

4 MODE SELECTION ALGORITHM

We here propose a new mode selection algorithm combining the recently develop mode selection and error estimation methods [17, 20]. The proposed new mode selection algorithm will be compared with another mode selection algorithm using frequency cut-off rule. To distinguish those two algorithms, we here use "eigenvector based mode selection algorithm (E-MSA)" and "frequency cut-off mode selection algorithm (F-MSA)". The sequential procedures of these mode selection algorithms are summarized in Tables 1 and 2.

Step 1. Initial preparation

(a) $\mathbf{M}_g$ and $\mathbf{K}_g$ are given.

(b) The range of the target global modes is determined: N_t^L and N_t^U.

(c) Error tolerance ε is assigned.

(d) $\overline{N}_d$ is determined for the reduced models.

Step 2. Construction of the reduce model

(a) The substructural eigenvalue problem are solved: $[\mathbf{K}_s^{(k)} - \lambda_i^{(k)} \mathbf{M}_s^{(k)}](\boldsymbol{\varphi}_s^{(k)})_i = \mathbf{0}$, for $k = 1,2,...,N_s$.

(b) The dominant substructural modes are selected by the frequency cut-off rule.

(c) The reduced model is constructed and solved: $\overline{\mathbf{K}}_p (\overline{\boldsymbol{\varphi}}_p)_i = \overline{\lambda}_i \overline{\mathbf{M}}_p (\overline{\boldsymbol{\varphi}}_p)_i$.

Step 3. Convergence check

(a) Relative eigenvalue error is estimated using Equation (16).

(b) Convergence is check in target range: $\eta_i \le \varepsilon$ $(N_t^L \le i \le N_t^U)$.

If the target eigenvalues have converged, stop.

Otherwise, continue.

(c) Increase the number of retained modes:

$\overline{N}_d = \overline{N}_d + 1$.

(d) Go to step 2(b).

Table 1: Frequency cut-off mode selection algorithm.

Step 1. Initial preparation

(a) $\mathbf{M}_g$ and $\mathbf{K}_g$ are given.

(b) The range of the target global modes is determined: N_t^L and N_t^U.

(c) Error tolerance ε is assigned.

(d) $\tilde{N}_d$ and $\overline{N}_d$ are determined for the intermediate and final reduced models, respectively.

Step 2. Construction of the intermediate reduced model

(a) The substructural eigenvalue problem are solved: $[\mathbf{K}_s^{(k)} - \lambda_i^{(k)}\mathbf{M}_s^{(k)}](\boldsymbol{\varphi}_s^{(k)})_i = \mathbf{0}$, for $k = 1,2,...,N_s$.

(b) The dominant substructural modes are selected by the frequency cut-off rule for the intermediate reduced model.

(c) The intermediate reduced model is constructed $\tilde{\mathbf{M}}_p$ and $\tilde{\mathbf{K}}_p$.

Step 3. Construction of the final reduce model

(a) The intermediate eigenvalue problem is solved and $\tilde{\boldsymbol{\Phi}}_{q_d}$ is found: $\tilde{\mathbf{K}}_p(\tilde{\boldsymbol{\varphi}}_p)_i = \tilde{\lambda}_i\tilde{\mathbf{M}}_p(\tilde{\boldsymbol{\varphi}}_p)_i$.

(b) The substructural modal contributions $C_i^{(k)}$ are calculated using Equation (9) in the target range $N_t^L \sim N_t^U$.

(c) The dominant modes are selected using $C_i^{(k)}$ for the final reduced model.

(d) Final reduced model is constructed and solved: $\overline{\mathbf{K}}_p(\overline{\boldsymbol{\varphi}}_p)_i = \overline{\lambda}_i\overline{\mathbf{M}}_p(\overline{\boldsymbol{\varphi}}_p)_i$.

Step 4. Convergence check

(a) Relative eigenvalue error is estimated using Equation (16).

(b) Convergence is check in target range: $\eta_i \le \varepsilon$ ($N_t^L \le i \le N_t^U$).

If the target eigenvalues have converged, stop.

Otherwise, continue.

(c) Increase the number of retained modes: $\overline{N}_d = \overline{N}_d + 1$.

(d) Go to step 3(c).

Table 2: Eigenvector based mode selection algorithm.

5 NUMERICAL EXAMPLES

We consider a cylindrical shell problem modeled by 24×24 MITC4 shell finite elements [23-25], and the free boundary condition is imposed. Length L is 12m, radius R is 0.5m, and thickness h is 0.005m. Young modulus is 69GPa, Poisson's ratio is 0.35, and structural density is $2700\,kg/m^3$. The cylindrical shell is partitioned into two substructures ($N_s = 2$), see Figure 1.

Performances of the mode selection and error estimation methods are tested in the target global range with $N_t^L = 5$ and $N_t^U = 15$. 70 substructural modes are retained for the intermediate reduced model ($\tilde{N}_d = 200$). Figures 2 and 3 show the performance of the mode selection and error estimation methods employed in this work. Also, we test the performance of E-MSA compared with F-MSA. 20 substructural modes are initially retained ($\overline{N}_d = 15$), and error tolerance ε is assigned by 10^{-3}. Using E-MSA, total modes in the target range converge much faster than F-MSA, see Table 3 and Figure 4.

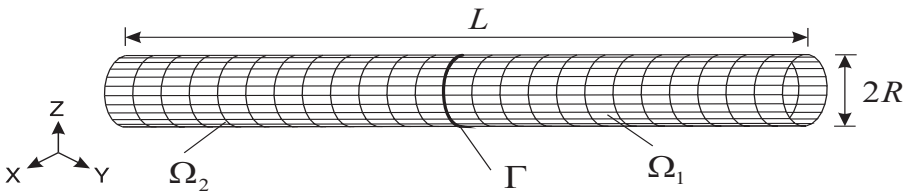

Figure 1: Cylindrical shell problem.

	Total number of iteration	Final number of retained substructural mode
E-MSA	8	28
F-MSA	52	72

Table 3: Numbers of iteration and retained mode.

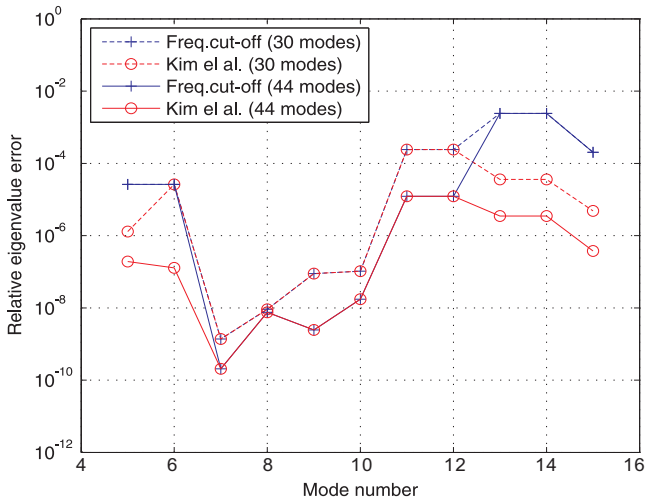

Figure 2: Relative eigenvalue error.

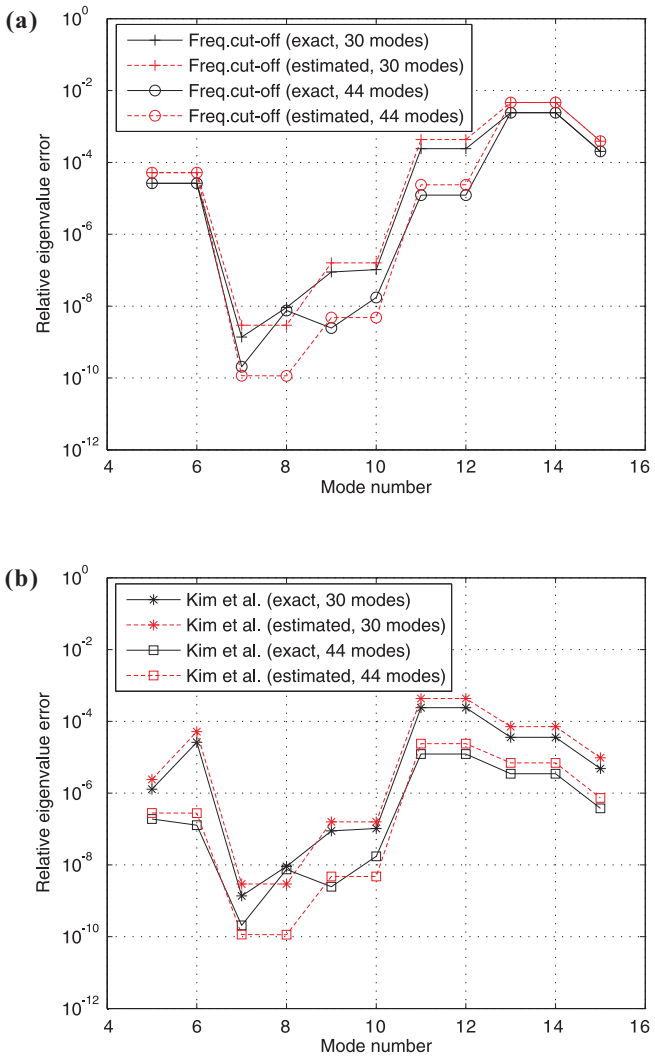

Figure 3: Exact and estimated relative eigenvalue errors. (a) Frequency cut-off rule, and (b) Kim et al. [17].

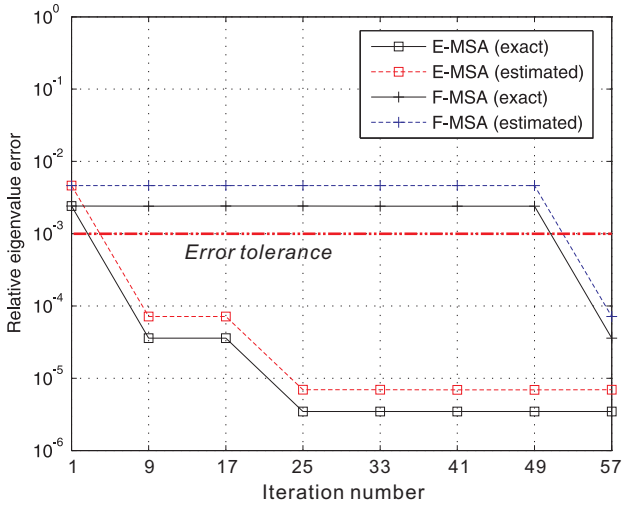

Figure 4: Convergence curve of the 14th mode.

6 CONCLUSIONS

We here propose a new mode selection algorithm in the F-CMS method, and then recently developed robust mode selection and error estimation methods are employed [17, 20]. The proposed mode selection algorithm was compared with the conventional mode selection algorithm using the frequency cut-off rule. We first reassessed the mode selection and error estimation methods, and then tested performance and features of the proposed mode selection algorithm using cylindrical shell problem. Those results show the excellent performance of the proposed mode selection algorithm. Although it is only studied in the F-CMS method here, this idea could be applicable to other CMS methods.

ACKNOWLEDGMENTS

This research was supported by Basic Science Research Program through the National Research Foundation of Korea (NRF) funded by the Ministry of Science, ICT & Future Planning (No. 2014R1A1A1A05007219).

REFERENCES

[1] W. Hurty, Dynamic analysis of structural systems using component modes. *AIAA Journal*, **3**(4), 678-685, 1965.

[2] R. Guyan, Reduction of stiffness and mass matrices. *AIAA Journal*, **3**(2), 380, 1965.

[3] R.R. Craig, B.C.C. Bampton, Coupling of substructures for dynamic analysis. *AIAA Journal*, **6**(7), 1313-1319, 1968.

[4] R.H. MacNeal, Hybrid method of component mode synthesis. *Computers & Structures*, **1**(4), 581-601, 1971.

[5] W.A. Benfield, R.F. Hruda, Vibration analysis of structures by component mode substitution. *AIAA Journal*, **9**, 1255-1261, 1971.

[6] S. Rubin, Improved component-mode representation for structural dynamic analysis. *AIAA Journal*, **13**(8), 995-1006, 1975.

[7] J.K. Bennighof, R.B. Lehoucq, An automated multilevel substructuring method for eigenspace computation in linear elastodynamics. *SIAM Journal on Scientific Computing*, **25**(6), 2084-2106, 2004.

[8] D.J. Rixen, A dual Craig-Bampton method for dynamic substructuring. *Journal of Computational and Applied Mathematics*, **168**(1-2), 383-391, 2004.

[9] D.D. Klerk, D.J. Rixen, S.N. Voormeeren, General framework for dynamic substructuring: history, review, and classification of techniques. *AIAA Journal*, **46**(5), 1169-1181, 2008.

[10] J.G. Kim, S.H. Boo, P.S. Lee, An enhanced AMLS method and its performance. *Computer Methods in Applied Mechanics and Engineering*, **287**, 90-111, 2015.

[11] J.G. Kim, P.S. Lee, An enhanced Craig-Bampton method, *International Journal for Numerical Methods in Engineering*, 03/2015; DOI: 10.1002/nme.4880.

[12] K.C. Park, Y.H. Park, Partitioned component mode synthesis via a flexibility approach. *AIAA Journal*, **42**(6), 1236-1245, 2004.

[13] D. Markovic, K.C. Park, A. Ibrahimbegovic, Reduction of substructural interface degrees of freedom in flexibility-based component mode synthesis. *International Journal of Numerical Methods in Engineering*, **70**, 163-180, 2007.

[14] K.C. Park, J.G. Kim, P.S. Lee, A mode selection criterion based on flexibility approach in component mode synthesis. *53th AIAA/ASME/ASCE/AHS/ASC Structures, Structural Dynamics, and Materials Conference*, Hawaii, USA, 2012.

[15] W.C. Hurty, A criterion for selecting realistic natural modes of a structure. *Technical Memorandum*, Jet Propulsion Laboratory, Pasadena, CA, 33-364, 1967.

[16] J.D. Collins, G.C. Hart, W.C. Hurty, B. Kennedy, Review and development of modal synthesis techniques. *Technical Report*, J. H. Wiggins, May 1972.

[17] J.G. Kim, P.S. Lee, K.C. Park, A mode selection method for accurate reduction of FE models in component mode synthesis. *Submitted to Computer Methods in Applied Mechanics and Engineering.*

[18] J.G. Kim, K.H. Lee, P.S. Lee, Estimating relative eigenvalue errors in the Craig‐Bampton method, *Computers & Structures*, **139**, 54-64, 2014.

[19] J.G. Kim, P.S. Lee, An accurate error estimator for Guyan reduction, *Computer Methods in Applied Mechanics and Engineering*, **278**, 1-19, 2014.

[20] J.G. Kim, P.S. Lee, A posteriori error estimation method for the flexibility-based component mode synthesis. *Submitted to AIAA Journal.*

[21] K. Elssel, H. Voss, An a priori bound for automated multilevel substructuring. *SIAM Journal on Matrix Analysis and Applications*, **28**(2), 386-397, 2007.

[22] H. Jakobsson, M.G. Larson, A posteriori error analysis of component mode synthesis for the elliptic eigenvalue problem. *Computer Methods in Applied Mechanics and Engineering*, **200**, 2840–2847, 2011.

[23] E.N. Dvorkin, K.J. Bathe, A continuum mechanics based four-node shell element for general nonlinear analysis. *Engineering Computations*, **1**(1), 77-88, 1984.

[24] H.M. Jeon, P.S. Lee, K.J. Bathe, The MITC3 shell finite element enriched by interpolation covers, *Computers and Structures*, **134**, 128-142, 2014

[25] Y. Lee, P.S. Lee, K.J. Bathe, The MITC3+ shell element and its performance, Computers and Structures, **131**(1), 12-23, 2014.